

# Structural Aspects and Surface Properties Molybdenum /Composite Oxide Catalysts

Mary Riad

GJRE Classification (FOR)  
090402

**Abstract-**Molybdenum / composite oxide catalysts play an important role in dehydrogenation – hydrogenation process. In the present investigation, alumina-magnesia and alumina-chromia composite materials were used as supports. The structural and phase changes of the prepared catalysts were confirmed using different techniques: Fourier transformer infrared spectroscopy, x-ray diffraction pattern, differential scanning calorimetry and surface properties. X-ray diffraction pattern exhibited the formation of  $MgMoO_4$  phase on the surface of alumina-magnesia support with small crystallite size. Bulky crystallites of  $MoO_3$  and  $Cr_2(MoO_4)_3$  were formed on alumina-chromia support. The thermal decomposition data emphasized the formation of  $Cr_2(MoO_4)_3$  (230-280°C),  $MoO_3$  (400-450°C) and  $MgMoO_4$  (350-500°C) phases. Surface properties indicate that, the bulky crystallites formed on the surface of alumina-chromia support, caused blocking of its pores and lead to an observed decrease in surface area from 240.2  $m^2/g$  for Mo/alumina-magnesia to 91.04  $m^2/g$  for Mo/alumina-chromia catalysts.

**Keywords-** Molybdenum, Support, Catalyst, Alumina, Magnesia, Chromia Composite mixed oxides.

## I. INTRODUCTION

Even though  $MoO_3$  as such is a very well-known catalyst due to its instability at higher temperature, it is often used in supported form. Supported molybdenum catalysts have been used in petroleum, chemical and pollution control industries, in addition to many industrial processes such as dehydrogenation hydrogenation and reforming<sup>(1)</sup>. Earlier alumina,  $TiO_2$ ,  $ZrO_2$ ,  $SiO_2$  and  $MgO$  were used as supports for molybdenum and studied their various physicochemical and catalytic properties<sup>(2,3)</sup>. It is a well-known fact that, in several catalytic reactions, catalysts supported on high surface area multicomponent oxide materials exhibit a better performance than when component oxides were used separately. It has been reported that high specific surface area molybdenum oxycarbide could be prepared from oxidative treatment of high surface area  $Mo_2C$  or low surface area  $MoO_3$ <sup>(4,5)</sup> and or by slurry impregnation of molybdenum salt on activated carbon<sup>(6)</sup>. Daturi et al.,<sup>(7)</sup> showed that high surface area  $Mo/SnO_2$  catalyst was very active catalyst for the oxidative dehydrogenation of alcohols; it showed higher activity than  $Mo/TiO_2$ ,  $Mo/Al_2O_3$  and  $Mo/SiO_2$  catalysts. Armaroli et al.,<sup>(8)</sup> explored an alternative way to prepare  $Mo/Al_2O_3$  catalyst by impregnation of molybdenum onto boehmite and then transformed it to  $MoO_3$ /alumina, the catalyst showed high

surface area. Mixed oxide supports showed also high surface area and peculiar behavior compared to the original pure oxides. These due to the combination of dissimilar components in the same molecular network structure. Cadus et al.,<sup>(9)</sup> prepared molybdenum supported on alumina-magnesia mixed oxide and found that,  $MgMoO_4$  system provided high selectivity to propene. It has been pointed out that, the presence of  $MoO_3$  helps in increasing the catalytic activity of molybdenum catalysts. Kumar et al.,<sup>(10)</sup> prepared a series of molybdenum loading from 2 to 14 wt% on  $Al_2O_3$ - $MgO$  mixed oxide by incipient wetness impregnation. The results indicated that, the presence of  $MoO_3$  species further enhanced the acidity of catalyst favorable for hydrocracking. Some authors demonstrated that magnesium molybdate exhibited higher selectivity toward olefin formation compared with magnesium vanadate system. Each of these described an improvement in the catalytic activity of  $MgMoO_4$  system with slight excess of molybdenum species<sup>(11,12)</sup>. Several molybdenum containing hydrotalcite like compound were prepared by different ionic exchange procedure using as parent synthetic hydrotalcite. The catalysts showed higher activity towards hydrogenation reaction<sup>(13,14)</sup>. This work concerned on studying the nature of molybdenum species on previously prepared alumina, alumina-magnesia and alumina-chromia composite mixed oxides. Emphasis was placed on the physicochemical characterization of the prepared catalysts with the aim of studying the nature of active sites and surface properties.

## II. EXPERIMENTAL

### A. Preparation of Composite Support

$\gamma$ - Alumina,  $\gamma$ -alumina-magnesia and  $\alpha$ -alumina-chromia composite mixed oxide support was previously prepared<sup>(14)</sup> via co-precipitation technique and followed by calcination at 450°C for alumina and alumina-magnesia & at 600°C for alumina-chromia composite materials.

### B. Preparation of Catalyst

The catalysts were prepared by incipient wet impregnation technique, in which the prepared composite supports were impregnated with ammonium heptamolybdate solution at pH ~ 12 using ammonium hydroxide to prepare the corresponding catalysts. The prepared catalysts dried at 120°C and then calcined in presence of flow of purified air. The calcination was performed in two steps, firstly from ambient temperature to 450°C, maintained at this temperature for two hours, and then calcined at 600°C for

six hours. The amount of ammonium heptamolybdate was equivalent to 20wt% MoO<sub>3</sub> loading.

### C. Structural Phase changes

The prepared catalysts were characterized by applying different techniques such as; Fourier transformer infrared spectroscopy, run on Perkin Elmer FT-IR apparatus, to identify the hydroxyl and the functional groups containing the catalysts. X-ray diffraction pattern, was carried out using XD-D1 – x-ray diffraction Shimadzu apparatus, to study the crystalline phases and the crystallite size using Sherrer's equation. Differential Scanning Calorimetry analysis was carried out using the Differential Thermal Analyzer, Perkin Elmer apparatus, to identify the different oxide phases formed upon thermal treatment. In addition, nitrogen physisorption isotherms, was measured to calculate surface area from adsorption curve by BET method.

### D. Surface Acidity

A Boehm's base neutralization technique<sup>(15)</sup> was used for measuring the surface acidity of the prepared catalysts. In this technique, 0.2 gm of sample was mixed with 100 ml of 0.1N NaOH solution and maintained overnight at room temperature. The mixture left to settle then filtered. The excess base (NaOH) was back titrated with standard solution of 0.1N HCl. Boehm concluded that NaOH neutralize the acidic groups and therefore measure the total surface acidity of the prepared catalysts.

## III. RESULTS and DISCUSSION

### a) FT-IR Spectroscopy

FT-IR spectra for  $\gamma$ -alumina, molybdenum/alumina and thermal treated molybdenum/alumina, molybdenum/alumina-magnesia & molybdenum/alumina-chromia catalysts were recorded at range from 2000-400 cm<sup>-1</sup> and extended FT-IR spectra at 3800-3200 cm<sup>-1</sup>. Data in Figure (1-a) reflected the appearance of band

at 1050 cm<sup>-1</sup>, that was typically for  $\gamma$ -alumina due to Al-O vibration mode. In addition, five bands in the OH stretching region 3800-3400 cm<sup>-1</sup> are appeared: a weak shoulder band at 3790 cm<sup>-1</sup> related to the terminal OH over one tetrahedrally coordinated aluminum ion in non-vacant environment, band at 3775 cm<sup>-1</sup> ascribed to the terminal OH over one tetrahedrally coordinated aluminum ion near a cation vacancy, band at 3735 cm<sup>-1</sup> related to terminal OH over one octahedrally coordinated Al ion, band at 3670 cm<sup>-1</sup> related to the bridging OH and band at 3590 cm<sup>-1</sup> related to the triply bridging OH. Meanwhile, band appeared at 3570 cm<sup>-1</sup> assigned to stretching modes of physisorbed water (hydrogen-bonded hydroxyl water)<sup>(16, 17)</sup>. Figure (1-b) ascribed one broad band, at 950 cm<sup>-1</sup>, that can be observed for molybdenum/alumina catalyst. This band attributed to Mo-O stretching. Ono et al,<sup>(18)</sup> studied the system Mo-Zr and suggesting that band appeared at 960 cm<sup>-1</sup> is related to superficial Mo species supported on ZrO<sub>2</sub> and suggesting that it resulted from the shifting of Mo-O bond stretching. Kaztelan et al.,<sup>(1)</sup> used raman spectra to characterize Mo/Al<sub>2</sub>O<sub>3</sub> catalyst with intermediate molybdenum loading and attributed the appearance of band in the range 941-947 cm<sup>-1</sup> to heptamolybdate species Mo<sub>7</sub>O<sub>24</sub><sup>-2</sup>. Desikan et al,<sup>(19)</sup> employing also raman spectra and observed that the vibration band around 960-950 cm<sup>-1</sup> in Mo/Al<sub>2</sub>O<sub>3</sub> and Mo/TiO<sub>2</sub> to dispersed isopolymolybdate and hydrated tetrahedral dioxo species. Accordingly, the same type of bond and similar coordination characterize these Mo species on that their vibrational spectra should be similar in accordance in these observations, the band at 955 cm<sup>-1</sup> is attributed to polymolybdate species dispersed on the surface. Band appeared at 3210 cm<sup>-1</sup> was typical for N-H bond vibration of ammonium salt used during the preparation. Acidic hydroxyl group for  $\gamma$ -alumina (at 3670 cm<sup>-1</sup>) is still appeared; meanwhile the most basic and basic hydroxyl group at 3775 & 3735 cm<sup>-1</sup> are disappeared. This ensures the complete interaction of molybdenum species with basic alumina hydroxyl groups.

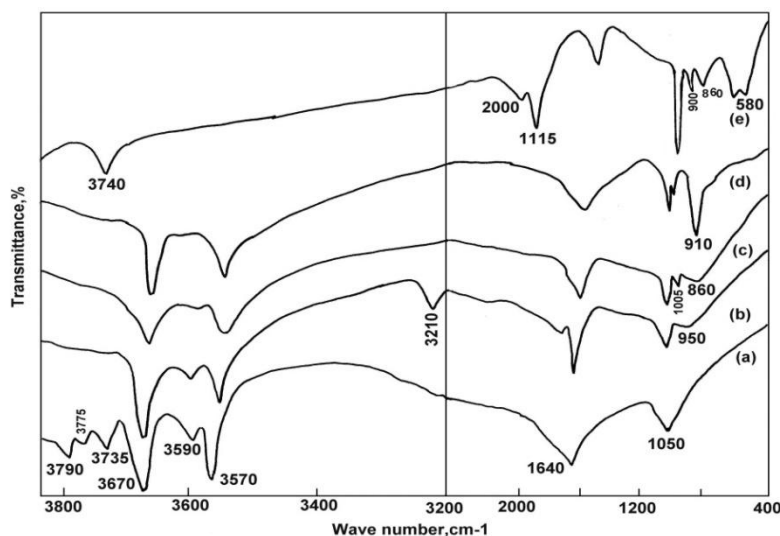


Fig. (1): FT-IR Spectra of: (a)  $\gamma$ -Alumina (b) Molybdenum/alumina (c) Molybdenum/alumina\* (d) Molybdenum/alumina-magnesia\* (e) Molybdenum/alumina-chromi

### b) calcined catalysts

Segawa et al, <sup>(20)</sup> reported, molybdenum reacts with basic and neutral OH group of support and suggest the creation of Mo isolated species have tetrahedral coordination. Okmoto and Imanaka <sup>(21)</sup> observed that, molybdate anion reacts with most and moderate basic hydroxyl group at 3775 & 3735  $\text{cm}^{-1}$  and these basic hydroxyl groups are the preferred interaction sites for the molybdate anion. In addition, the disappearance of these bands indicated that both OH groups are involved in the interaction with the same molybdate species i.e. bidentate chain like structure is formed. After calcination of molybdenum/alumina catalyst (Fig.1-c), band at 950  $\text{cm}^{-1}$  is disappeared and another new feature appeared at 860 and 1005  $\text{cm}^{-1}$ . These modifications have been previously observed for Mo supported on different oxide <sup>(22,23)</sup> and it has been explained by structural alterations in Mo species. According to Deskain et al, <sup>(19)</sup> this phenomenon would indicate on the presence of isolated tetrahedral Mo species that are present in octahedral coordination in the presence of water. Giordano et al, <sup>(22)</sup> have proposed that, at low Mo concentration (< 2%  $\text{MoO}_3$ ), tetrahedrally coordinated  $\text{MoO}_4^{2-}$  are present and that at moderate loading (4-20%  $\text{MoO}_3$ ), both tetrahedrally and octahedrally coordinated MoOx species are present. Chen et al, <sup>(23)</sup> reported the same conclusion. The vibration at 860  $\text{cm}^{-1}$  may be associated with Mo-O-Mo or due to Mo-O-Al bonds, as investigated by Okamoto et al, <sup>(21)</sup>. Actually, band at 1005  $\text{cm}^{-1}$  attributed to crystalline  $\text{MoO}_3$  <sup>(20)</sup>. This band associated the vibration of Mo=O in  $\text{MoO}_3$  and Mo-O-Al in aluminum molybdate phases. Whereby, the disappearance of bands at 3210 and 950  $\text{cm}^{-1}$  accompanied the decomposition of ammonium heptamolybdate on thermal treatment. For calcined molybdenum/alumina-magnesia catalyst, band appeared at 910  $\text{cm}^{-1}$  ascribed to magnesium molybdate, in addition to band assigned to  $\text{MoO}_3$  species (at 1005  $\text{cm}^{-1}$ , Fig.1-d). The spectrum for calcined molybdenum/alumina-chromia catalyst, in Fig. (1-e) presented the appearance of, band at 900  $\text{cm}^{-1}$  that assigned to vibration of Mo-O-Cr in molybdenum dichromate, band at 2000  $\text{cm}^{-1}$  assigned to chromate vibration and band at 850  $\text{cm}^{-1}$  assigned to Cr-O-Cr vibration <sup>(24)</sup>. Band appeared at 580  $\text{cm}^{-1}$  typical of  $\text{Cr}^{+3}$  polymeric species, also this band assigned to Cr-O vibration with octahedrally distorted coordination of Cr atoms in  $\text{Cr}_2\text{O}_3$  crystallites <sup>(25,26)</sup>, in addition to  $\text{MoO}_3$  band. Band appeared at 1115  $\text{cm}^{-1}$  has been interpreted as due to bulk tetrahedrally Al-O stretching of  $\alpha$ -alumina. In addition, band appeared at 3740  $\text{cm}^{-1}$  related to bridged OH group and terminal octahedral OH group with vacancy and this is typical for  $\alpha$ -alumina. The presence of chromia species facilitated transformation of  $\gamma$ - form to  $\alpha$ - one at lower temperature "600°C" via sintering effect. Benitez et al, <sup>(27)</sup> reported that, the concentration of tetrahedrally coordinated molybdenum species strongly interacted with  $\gamma$ -alumina is

decreased upon changing  $\gamma$ -alumina to  $\alpha$ - form; meanwhile, the concentration of low interacted octahedrally coordinated molybdenum oxide species is increased.

### c) X-ray Diffraction Pattern

X-ray diffraction pattern (XRD) for all the prepared and calcined catalysts are depicted in the Figs. (2-4). For molybdenum/alumina catalyst, the diffractogram in Fig.2-a, revealed the appearance of broad peaks characterized  $\gamma$ -alumina at d spacing: 2.41, 1.98 and 1.40 Å, (ASTM 04-0875). Molybdenum species in ammonium heptamolybdate detected at d- spacing

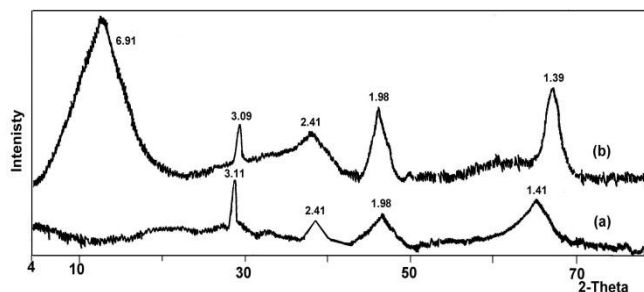


Fig.(2): X-ray Diffraction Pattern of: (a) Molybdenum/alumina (b) Molybdenum/alumina\*

3.85, 3.11 and 1.85 Å <sup>(28,29)</sup>. Figure (2-a) revealed the appearance of line at d-spacing: 3.11 Å with low intensity, the other two lines may be shielded upon incorporation of molybdenum species inside alumina pores. Diffractogram for calcined molybdenum/alumina-magnesia (Fig. 2-b), exhibited broad peaks at d-spacing 6.91, 3.09 and 2.41 Å that related to formation of  $\text{Al}_2(\text{MoO}_4)_3$  phase <sup>(29)</sup>. Zingg et al, <sup>(30)</sup> reported that, the diffusion of Mo cation into the support during the calcination step leading to a well-defined Al-molybdate. Wachs et al, <sup>(31)</sup> concluded that, Mo chemically adsorbed on the surface of alumina through the formation of Mo-O-Al bond yielding to superficial molybdate species. The broadening of aluminum molybdate peaks with slight high intensities related to that aluminum molybdate had relative large crystallite size to be detected by XRD and may be distorted <sup>(29,30)</sup>. No lines were detected for presence of  $\text{MoO}_3$  phase that may be formed with small amount and highly dispersed within the support surface. For molybdenum/alumina-magnesia catalyst (Fig.3a), lines are detected at d-spacing 2.43, 2.02 and 1.42 Å characterized alumina-magnesia composite <sup>(30)</sup>, in addition to that related to molybdenum species. After thermal treatment, x-ray diffraction pattern in Fig.3-b, revealed the appearance of lines at d-spacing 3.39, 2.08 and 1.43 Å where  $\text{MgMoO}_4$  phase was characterized by presence of these principal lines <sup>(31)</sup>. Thus, molybdenum reacted preferably with magnesia component of the support and formed very stable crystallites of  $\text{MgMoO}_4$

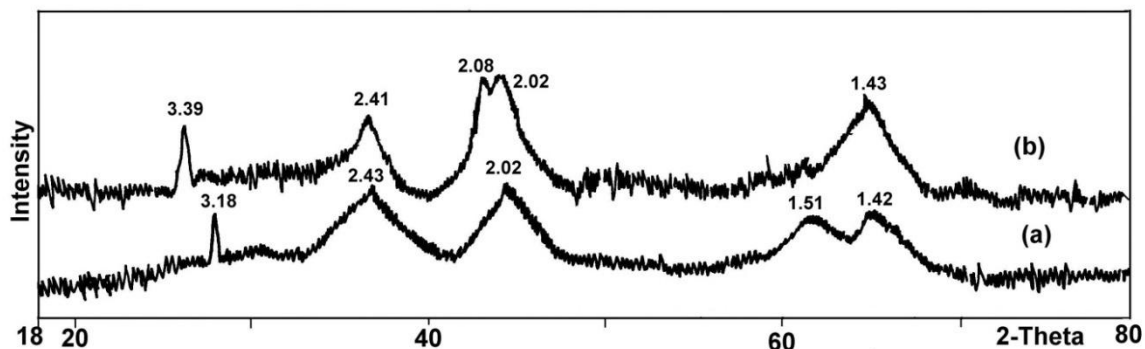


Fig.(3): X-ray Diffraction Pattern of: (a) Molybdenum/alumina-magnesia  
(b) Molybdenum/alumina – magnesnia

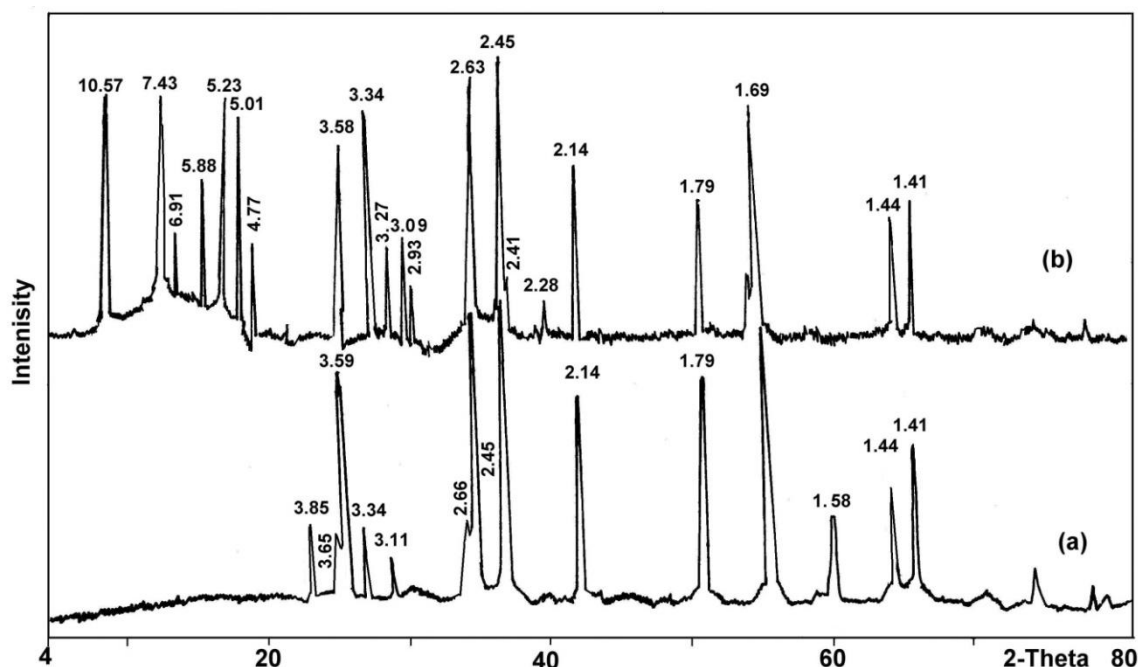


Fig.(4): X-ray Diffraction Pattern of: (a) molybdenum/alumina-chromia  
(b) molybdenum/alumina – chromia

The broadening of the peaks may be suggested that magnesium molybdate was distorted. In addition, no lines were detected for presence of  $\text{MoO}_3$  phase. Jolly et al, <sup>(32)</sup> indicated that, a considerable amount of  $\text{MgO}$  was hydrolyzed to  $\text{Mg}(\text{OH})_2$  upon impregnation with ammonium heptamolybdate salt solution, and this reacted with  $\text{Mo}_7\text{O}_{24}^{6-}$  to  $\text{MgMoO}_4$ . When this catalyst heated at  $600^\circ\text{C}$  in presence of air,  $\text{MgMoO}_4$  was identified in XRD as reported by Stampfi et al <sup>(33)</sup>. For molybdenum/ alumina-chromia catalyst (Fig.4-a), lines detected at d-spacing : 3.65, 2.66 and 1.69 Å corresponded to  $\text{Cr}_2\text{O}_3$  phase <sup>(34)</sup> and that detected at d-spacing : 3.59, 2.63 and 1.79 Å were corresponding to the presence of  $\alpha$ -alumina <sup>(35)</sup>, in addition to lines detected for presence of molybdenum species (d-spacing: 3.85, 3.11 and 1.58 Å). Diffractogram for calcined molybdenum/alumina-chromia catalyst (Fig. 4-b), revealed

the appearance of new lines at d-spacing: 7.43, 5.88 and 2.93 Å corresponded to  $\text{Cr}_2(\text{MoO}_4)_3$  phase. Lines detected at d-spacing 5.01, 5.23 and 4.77 Å assigned to molybdenum dichromate phase <sup>(36, 37)</sup>. In addition, lines detected at 10.57, 3.27 and 2.28 Å related to  $\text{MoO}_3$  phase and that at d-spacing: 6.91, 3.09 2.41 Å related to  $\text{Al}_2(\text{MoO}_4)_3$  phase formation <sup>(29, 30)</sup>.

#### d) Crystallite size

Crystallite size data for the prepared catalysts before and after calcination were included in Table (1). Data indicated that, the crystallite size had relatively low values (7.0, 10.6 nm) for molybdenum/alumina–magnesia catalyst. This may be due to the presence of relatively smaller particles of basic magnesia comparing with competitive alumina particles that

allowed the dispersion of molybdenum species and consequently prevented their aggregation.

On the other hand, the crystallite for molybdenum/alumina-chromia catalyst, showed high values (47.0 and 44.9 nm). The higher value for such catalyst was owing to the presence of large acidic  $\text{Cr}_2\text{O}_3$  ( $2\text{Cr}^{+3} 3\text{O}^{-2}$ ) species which induced attraction forces between the different particles and permitted the aggregation of molybdenum species. In addition, the blooming of  $\alpha$ -alumina increases crystallite size quickly, that means the formation of  $\alpha$ -alumina accompanied by exaggerated grain growth.

**Table (1): Crystallite Size for Prepared Molybdenum Catalysts.**

2 $\theta$	Mo/alumina	Mo/alumina-magnesia	Mo/alumina-chromia
28.9	36.89	----	----
36.79	23.36	7.00	47.00
41.9	----	----	44.90
44.79	----	10.60	----
2 $\theta$	Mo/alumina*	Mo/alumina-magnesia*	Mo/alumina-chromia*
36.6	28.26	6.1	38.5
41.97	----	----	86.5
45.6	19.2	4.9	----

After thermal treatment, the crystallite size data showed the same trend as that obtained for the previous prepared catalysts. This ensures that alumina-magnesia support prevented the formation of large molybdenum oxide particles and facilitated the dispersion of the formed magnesium molybdate phase on its surface, as clarified from XRD data. Concurrently, for calcined molybdenum/alumina-chromia, different chromium-molybdenum phases were formed on the surface of alumina-chromia support; these species were migrated and agglomerated together to form bulky crystallites with size of, 38.5 and 86.5 nm or these phases may form a strongly packed layer cracks as a result of crystallite growth.

#### e) Base Neutralization

Applying Boehm's base neutralization technique<sup>(15)</sup> for measuring the surface acidity of the prepared molybdenum catalysts, data is included in Table (2). Data clarified that the alumina-magnesia support exhibited the lowest surface acidity as compared with the other two supports.

**Table (2): Surface Acidity for Prepared Molybdenum Catalysts.**

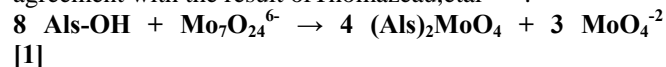
Sample	Al <sub>2</sub> O <sub>3</sub>	Al <sub>2</sub> O <sub>3</sub> -MgO	Al <sub>2</sub> O <sub>3</sub> -Cr <sub>2</sub> O <sub>3</sub>	Mo/Al <sub>2</sub> O <sub>3</sub> -MgO*	Mo/Al <sub>2</sub> O <sub>3</sub> -Cr <sub>2</sub> O <sub>3</sub> *
Acidity (meqv/100.gm <sup>1</sup> )	22.3	8.5	26.0	27.0	14.7

For the corresponding catalysts, the same trend was observed. In other words, calcined molybdenum/alumina-magnesia catalyst was the lowest one i.e. the presence of basic MgO limited the acidity of molybdenum/alumina-magnesia catalyst. The catalyst that had high surface acidity was molybdenum/alumina-chromia.

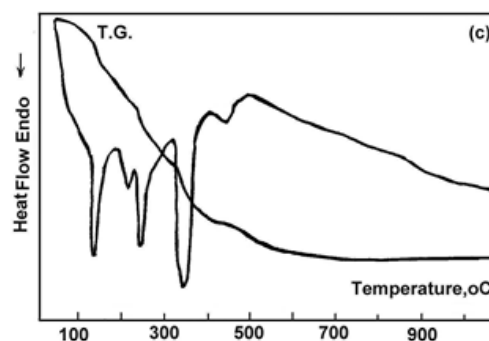
#### f) Differential Scanning Calorimetry

Differential scanning calorimetry (DSC) profiles for the prepared catalysts represented in Fig (5). For molybdenum/alumina catalyst (Fig.5-a), three endothermic peaks appeared, the first at temperature range 100-180°C related to the removal of surface adsorbed water. The second peak appeared at temperature range 400-450°C related to the decomposition of  $(\text{NH}_4)_6\text{Mo}_7\text{O}_{24} \rightarrow 7\text{MoO}_3 + 6\text{NH}_3 + 3\text{H}_2\text{O}$ , producing the corresponding oxide form<sup>(38)</sup>. The last one at 550-600°C corresponded to the formation of aluminum molybdate phase. Aluminum molybdate is a thermodynamically stable phase and has been reported to form in high loading at temperature  $\sim 600^\circ\text{C}$ . Cheng and Scharader<sup>(39)</sup> have shown that aluminum molybdate is not formed when molybdenum/alumina catalyst is calcined at 550°C even though the  $\text{MoO}_3$  content is 20 wt%.

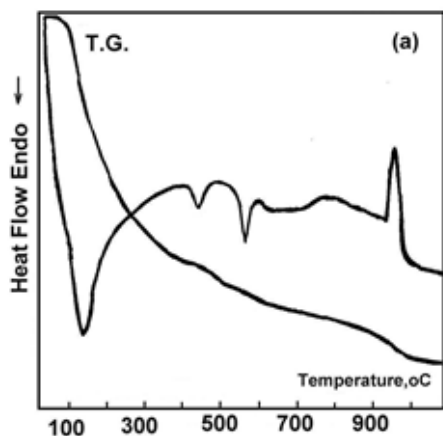
The heat of absorption (enthalpy) for this peak is shown to be low value 3.87  $\mu\text{V.s/mg}$  (Table 3), that indicated the easiest formation of polymolybdate species on the surface of amphoteric alumina support with its abundant OH groups, in agreement with the result of Thomazeau, et al<sup>(40)</sup>.



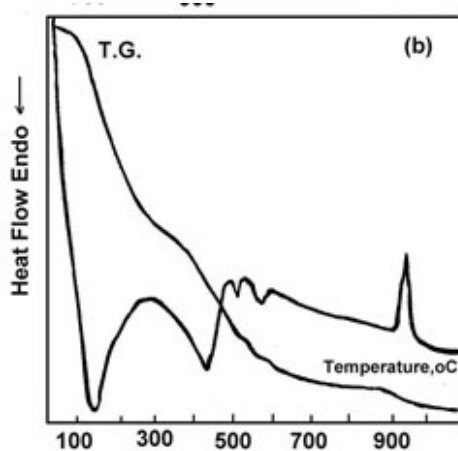
An exothermic peak appeared at temperature range 950-1000°C, related to transformation of  $\gamma$ -alumina to  $\alpha$ -form<sup>(1)</sup>.



**Molybdenum/alumina**



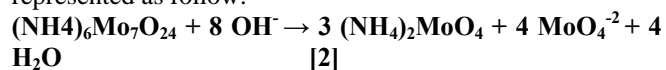
Molybdenum/alumina-magnesia



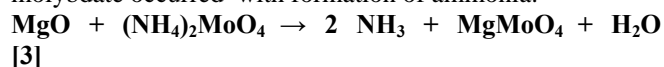
Molybdenum /alumina-chromia

For molybdenum/alumina-magnesia catalyst, DSC profile (Fig.5-b) revealed a new endothermic peak in addition to the surface adsorbed water,  $\text{MoO}_3$  and aluminum molybdate phase peaks. This peak appeared at temperature range 350-500°C that related to formation of magnesium molybdate<sup>(29)</sup>, which co-existed with aluminum molybdate on the catalyst surface. As well known, alumina-magnesia support contained abundant of basic hydroxyl groups, that allowed depolymerization of polymolybdate anion yielding monomeric species anchored to the oxide surface.

The formation of ammonium mono-molybdate can be represented as follow:



under further heating, decomposition of ammonium mono-molybdate occurred with formation of ammonia:



As shown, strong base (MgO) replaced a weak one (ammonium species) in a molybdate salt and then basic OH group stabilized the highest  $\text{Mo}^{6+}$  oxidation state ( $\text{MgMoO}_4$ ). MgO is a strong basic support, high local pH of this support led to depolymerization of

polyoxomolybdates<sup>(41)</sup>. Therefore, most tetrahedral  $\text{MoO}_4$  moieties believed to be present in this catalyst. The low values of enthalpy: "4.67" for formation of magnesium molybdate species and "6.72  $\mu\text{V}\cdot\text{s}/\text{mg}$ " for aluminum molybdate ones (Table 3), indicate the easiest formation of these species. Radivan et.al,<sup>(42)</sup> reported that  $\text{MoO}_3$  formed on support reacted preferentially with magnesia to form magnesium molybdate at 500°C, and attributed the absence of all diffraction pattern of support as an indication for its complete transformation into  $\text{MgMoO}_4$ . The detection of  $\text{MoO}_3$  by IR and DSC analyses in this work is related to the unreacted  $\text{MoO}_3$  located far away from the composite surface that could highly inter dispersed among the  $\text{MgMoO}_4$  particles or over its surface. For molybdenum/alumina-chromia catalyst, four endothermic peaks appeared in addition to the surface water adsorption peak. The first at temperature range 200-230°C assigned to formation of molybdenum dichromate. The second and third endothermic peaks appeared at 230-280 and 280-380°C related to formation of chromium molybdate and molybdenum oxide respectively. The fourth one, at 420-500°C related to formation of aluminum molybdate phase. As well known, acidic support facilitated the formation of  $\text{MoO}_3$  bulk like particles beside the  $\text{MoO}_3$  clusters and polymolybdate species<sup>(41,42)</sup>. Enthalpy values were parallel to this behavior and showed a low values for the formation of these different oxide phases. As clarified, the temperature of ammonium heptamolybdate decomposition on alumina-chromia support was lower than that on alumina – magnesia one. This may be owing to the presence of acidic chromia species that hasten the decomposition of ammonium heptamolybdate at lower temperature. The endothermal effects as showed in the thermogravimetric curve (TG, Fig. 5 & Table3) accompanied the mass loss. This loss in weight resulted from the evolution of ammonia and H-bonded water, which may be attached either to already adsorb water molecule or to surface

**Table (3): Thermal Analysis of Molybdenum Catalysts**

Molybdenum/alumina			
Temperature <sup>o</sup> C	Type of peak	Enthalpy $\mu$ V.s/mg	Weight loss%
100-200	Endo-thermic	28.93	12.92
400-450	Endo-thermic	3.68	3.24
550-600	Endo-thermic	3.87	9.15
950-1000	Exo-thermic	-0.71	2.69
Molybdenum/alumina-magnesia			
Temperature <sup>o</sup> C	Type of peak	Enthalpy $\mu$ V.s/mg	Weight loss%
100-200	Endo-thermic	13.62	10.25
350-500	Endo-thermic	4.67	10.39
500-550	Endo-thermic	6.72	1.18
550-600	Endo-thermic	16.72	2.01
950-1000	Exo-thermic	-0.42	1.77
Molybdenum/alumina-chromia			
Temperature <sup>o</sup> C	Type of peak	Enthalpy $\mu$ V.s/mg	Weight loss%
100-180	Endo-thermic	13.33	12.92
200-230	Endo-thermic	0.67	5.56
230-280	Endo-thermic	6.72	13.71
280-380	Endo-thermic	26.06	17.62
420-500	Endo-thermic	0.84	6.81

hydroxyl groups. The weight losses accompanied the formation of  $\text{MoO}_3$  phase on either alumina or alumina-magnesia supports were low values, 3.24 and 1.18%, respectively. This is the reason for the impossibility of detection of  $\text{MoO}_3$  phase by XRD on these supports. Consequently, the support is not fully covered for molybdate layer and there is small amount of  $\text{MoO}_3$  on the support surface. Meanwhile, the weight loss accompanied the formation of  $\text{MoO}_3$  on alumina-chromia support is high value 17.62%, that is in agreement with Thomazeau, et. al, <sup>(40)</sup> who observed the decomposition of ammonium heptamolybdate on acidic silica and niobia ( $\text{Nb}_2\text{O}_5$ ), facilitated the formation

of bulky  $\text{MoO}_3$  and polymolybdate species, silicomolybdic acid could also be identified.

#### g) Surface Area and Pore Structure

Nitrogen isotherms were measured using Quantachrome Noava Automated Gas Sorption apparatus. Full nitrogen adsorption-desorption isotherms were obtained for molybdenum/alumina catalyst and that produced after thermal treatment of, molybdenum/alumina, molybdenum/alumina-magnesia and molybdenum/ alumina-chromia ones. Specific surface area ( $S_{\text{BET}}$ ), total pore volume ( $V_p$ ) and mean pore radius ( $r_H$ ), BET-C constant and fraction of micro porosity ( $m_f$  %) data were included in Table (4)

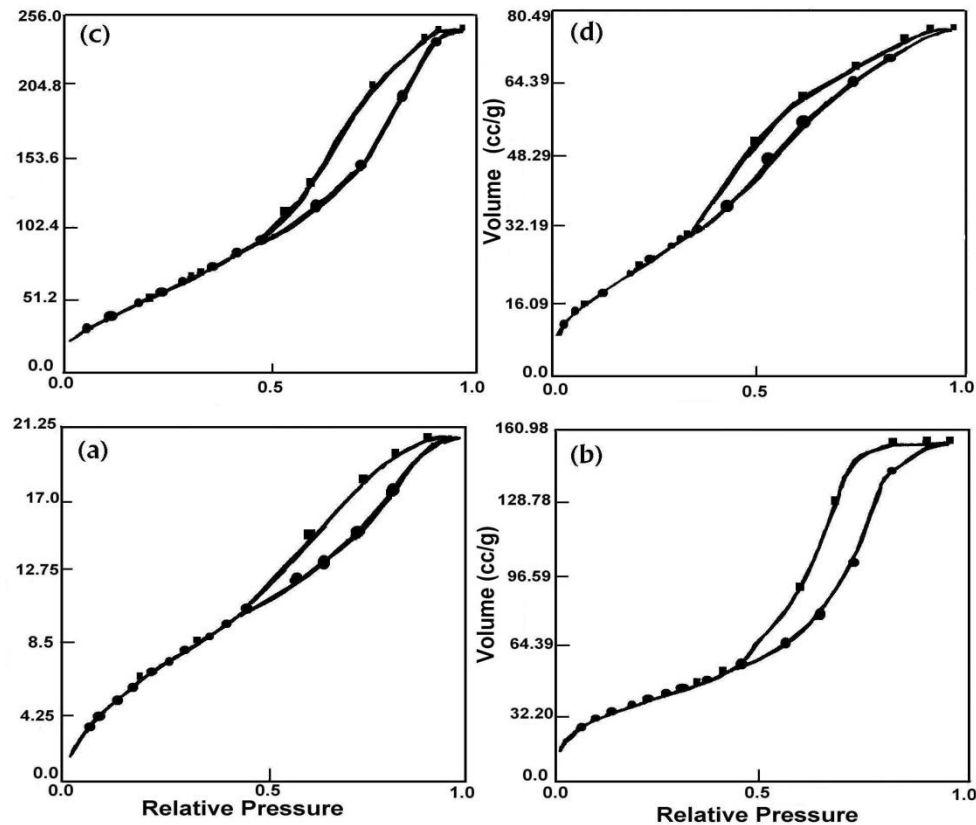


**Fig. (6):N<sub>2</sub> Adsorption Isotherm of: (a) Molybdenum/alumina (b)Molybdenum/alumina\* (c) Molybdenum/alumina – magnesia\* (d) Molybdenum/alumina – chromia**

All samples showed type IV isotherm of Brunauer classification according to IUPAC classification<sup>(43)</sup> and exhibited H2 hysteresis loop. This kind of hysteresis loop was an indication for a network of interconnected pores with narrower parts (Fig.6). The  $S_{BET}$  values for the calcined catalysts were computed from linear plots of the  $S_{BET}$  equation. The adsorption isotherm for molybdenum/alumina catalyst (Fig.6-a) showed small hysteresis and sharp decrease in surface area and pore volume as compared with  $\gamma$ -alumina support. This decrease resulted from; bulky crystallites of ammonium heptamolybdate blocked some of alumina narrower pores and also accumulated on the walls of the wider ones, giving rise to a decrease in all surface properties.

Thermal treatment at 450°C for molybdenum/alumina catalyst produced an increase in  $S_{BET}$  (from 24.95 to 133.6 m<sup>2</sup>/g), pore volume (from 0.0131 to 0.0713 cc/g), average pore radius (from 0.8016 to 1.400 nm) and microporosity % (from 9.9 to 16.87%). The effect was arising from the decomposition of incorporated ammonium heptamolybdate

into smaller molybdenum-oxygen entities with removal of ammonia that produced the observed changes.

For calcined molybdenum/alumina-magnesia catalyst, a further increase in surface area was observed from 133.6 for calcined molybdenum/alumina to 240.2 m<sup>2</sup>/g. This behavior indicated the modification of alumina-magnesia structure resulted from the interaction with molybdenum and formation of new oxide phases (in agreement with XRD and DSC data) which responsible for creation of new pores that contributed in the increase in surface area. Also, this increase is due to the formation of Mg(OH)<sub>2</sub> upon contact of MgO with water during incipient impregnation and its subsequent decomposition to high surface area MgO upon calcination, as reported by Mathew et al<sup>(44)</sup>. Meanwhile, accommodating molybdena particles in narrow pores cause some widening in these pores with an observable increase in pore volume. At the same time, some of these formed species may agglomerate inside narrow pores and block some of them with a result of decreasing pore radius and microporosity%, (Table 4).

**Table (4) : Surface Properties of the Prepared Catalysts**

Catalyst	BETC constant	S <sub>BET</sub> (m <sup>2</sup> /g)	S <sub>t</sub> (m <sup>2</sup> /g)	V <sub>p</sub> (cc/g)	r <sub>H</sub> (nm)	m <sub>f</sub> (%)
Alumina	65.04	170.80	164.54	0.0948	1.187	13.85
Mo/Alumina	28.06	24.95	15.64	0.0131	0.801	9.90
Mo/Alumina*	104.1	133.60	115.93	0.0713	1.400	16.87
Alumina-magnesia	73.36	209.7	233.37	0.1126	0.948	19.37
Mo/Alumina-Magnesia*	120.86	240.20	236.31	0.1880	1.050	13.80
Alumina-chromia	42.76	89.45	72.04	0.0504	0.891	16.25
Mo/Alumina-Chromia*	49.11	91.04	81.57	0.0507	0.831	18.24

\* is calcined catalysts

Concurrently, for calcined molybdenum/ alumina-chromia catalyst, surface area showed a low value 91.04 m<sup>2</sup>/g. This exactly related to formation of bulk crystallites of chromium and molybdenum oxide phases that covered different sites on the catalyst surface causing a blockage of pores and a decrease in surface area. In addition, the decrease in pore volume with the increase in m<sub>f</sub> % (as compared with molybdenum /alumina-magnesia catalyst) is related to: these bulk crystallites densely accumulated on support pore walls to diminish its radius and consequently the calculated microporosity % was shown to be high (Table 4). Nickolov et al.,<sup>(45)</sup> reported that, Mo-O entities are formed as tetrahedral monomeric MoO<sub>4</sub> and or octahedral polymeric - [MoO<sub>6</sub>]<sub>n</sub> surface species that interacted with chromium species formed bulk crystallites, in addition to bulk MoO<sub>3</sub> crystallites that caused semi blocking of alumina pores and provoked a decrease in surface area.

#### h) V<sub>t</sub>-t Plot

To analyze isotherm of materials containing micro- and mesoporosity, t-method of de Boer et al.,<sup>(46)</sup> was applied. The obtained S<sub>t</sub> values showed fair agreement with the

corresponding S<sub>BET</sub> values indicating a suitable choice of t-curves on the basis of the BET-C constant. For molybdenum/alumina catalyst, V<sub>t</sub>-t plot (Fig.7) showed downward deviation at t > 0.6 nm, thus the material was microporous one, but m<sub>f</sub> % showed to be lower value (Table 4). This situation was because of blocking and accumulation of ammonium heptamolybdate species inside alumina pores and caused a decrease in V<sub>p</sub> and r<sub>H</sub> values and then a sharp decrease in surface area was observed. In addition, a very low adsorption volume (Fig.7) was observed, this accompanied with blocking of most of micropores with ammonium heptamolybdate species and their accumulation inside alumina mesopores to produce and leave small size of pores to measure. Thus, the downward deviation was not a result of creation of new micro pores as observed by small value of m<sub>f</sub> %. After calcination, the material showed upward deviation because of destruction of ammonium heptamolybdate blocked the pores and removal of ammonia, in addition to the electrostatic repulsion created by charge adsorbed at the surface of particles. These two factors created an intracrystalline microporosity as clarified from the increase in m<sub>f</sub> % and pore volume.

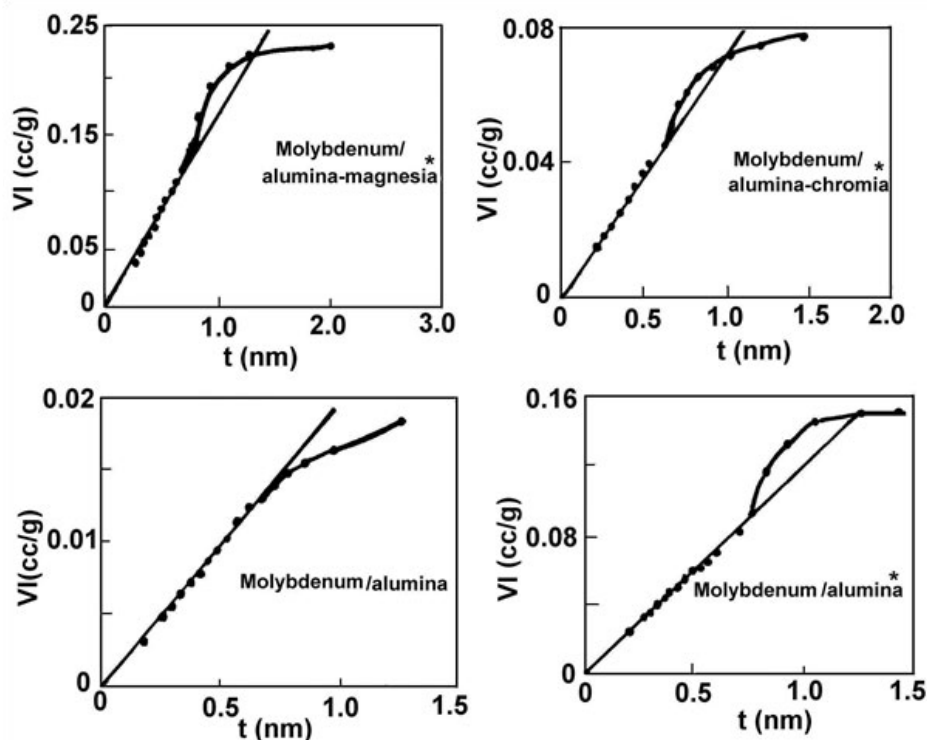


Fig. (7):  $V_t$ - $t$  Plot for the Prepared Catalysts

Calcined molybdenum/alumina –magnesia catalyst (Fig.7) showed also upward deviation (capillary condensation) characterized mesoporous materials at  $t > 0.8$  nm with high value of adsorbed volume i.e. thermal decomposition of ammonium heptamolybdate facilitates accommodation of mesopores in catalyst. The slight decrease in  $m_f\%$  and average pore radius and the increase in pore volume suggested generation of new deeper and slight wide mesopores that implies the dispersion of molybdenum species on support. Calcined molybdenum/alumina-chromia catalyst showed upward deviation at  $t > 0.6$  nm but with a relatively low value of adsorbed volume. The decrease in  $V_p$ ,  $r_H$  was explained on the aggregation of molybdenum inside support. Consequently, the increase in  $m_f\%$  suggested the shrinkage of many crystals during calcination which did not create internal porosity.

#### IV. CONCLUSION

From the results described above, it can be concluded that the preparation of Mo catalysts using different composite oxide supports allow formation of different phases as established by using different techniques:

X-ray diffraction pattern detected the formation of  $MgMoO_4$  active site on using alumina-magnesia support. This phase characterized by its small crystallite size. Bulky crystallites of different molybdenum-chromium oxide phases were formed on using alumina-chromia support.

Differential scanning calorimetry analysis suggested that the support chemistry was responsible for the decomposition of ammonium heptamolybdate, consequently on alumina-magnesia support, the presence of basic  $MgO$  facilitate its

decomposition and formation of magnesium molybdate. On other hand, its decomposition on alumina-chromia support ( $Cr_2O_3$  was acidic support) caused formation of bulk  $MoO_3$ , and polymolybdate species. Surface properties established that, the surface area of molybdenum/alumina-magnesia catalyst was the highest one compared with the other prepared catalysts.

#### Acknowledgement

I would like to submit my great thankfulness to *Prof. Dr. Sara Mikhail* Professor Doctor in Refining Department (EPRI) for her devotion, efforts and valuable guidance and discussion throughout this work.

#### V. REFERENCES

- 1) S. Kasztelan, E. Payen, H. Toulhoat, J. Grimblot, J. P. Bonnelle, Polyhedron 5 (1995) 157.
- 2) P. Sarrazin, S. Kasztelan, E. Payen, J.P. Bonnelle, J. Grimblot, J. Phys. Chem. 97 (1993) 5954.
- 3) M. Che, O. Clause, Ch. Marcilly, in : G. Ertl, H.Knozinger, J. Weitkamp,(Eds), Handbook of Hetrogenous Catalysis, vol. 1, VCH, weinheim, 1997, pp. 191-207.
- 4) A. Blekkan, C. Pham-Huu, M. J. Ledoux, J. Guille, Ind. Eng. Chem. Res. 33 (1994) 1657.
- 5) P. Del Gallo, F. Meumier, C. Pham-Huu, C. Crovzet, M. J. Ledoux, Ind. Eng. Chem. Res. 36 (1997) 4166.
- 6) X. M, J. Gong, X. Yng, S. Wang, Applied Catal. 280 (2005) 215.
- 7) M. Daturi, L. G. Appel, J. Catal. 209 (2002) 427.

- 8) T. Armaroli, D. Minoux, S. Gautier, P. Euzen, Appl. Catal. A. 251 (2003) 241.
- 9) L. E. Cadus, M. C. Abello, M. F. Gomez, J. B. Rivarola, Ind. Eng. Chem. Res. 35 (1996) 14.
- 10) M. Kumar, F. Aberuagba, J. K. Gupta, K. S. Rawat, L. D. Sharma, G. Muralishar, J. Mol. Catal. A. 213 (2004) 217.
- 11) N. Fujikawa, Y.S. Yoon, W. Ueda, Y. Moro-Oka, Trans. Mater. Res. Soc. Jpn. A. 15 (1994) 79.
- 12) L.E. Cadus, M.F. Gomez, M. C. Abello, Catal. Lett. 43 (1997) 229.
- 13) R. Zavocanu, R. Birjegnety, O. Sumitssu Pavel, A. Cruceenu, M. Alifnti, Appl. Catal. A 286 (2005) 211.
- 14) M. Riad, under publication.
- 15) H.P. Boehm, Adv. Catal. , 16 (1966) 79.
- 16) R.L. Mc Cormick, J.A. King, T.R. King , H.W. Haynes, Ind. Eng. Chem. Res. 28 (1989) 210.
- 17) Morterra, C. Emanuel, G. Cerrato, G. Magnacca, J.Chem. Soc. Faraday Trans. 88 (1992) 339.
- 18) T. Ono, H. Miyota, Y. Kubokawa, J. Chem. Soc. Faraday Trans, 83(1987) 1761.
- 19) N.Desikan, L. Huang, S.T. Oyama, J. Chem. Soc. Faraday Trans., 88(22)(1992) 3357.
- 20) K. Segawa, W. Hall, J.Catal., 76(1982) 133.
- 21) Y. Okamoto, T. Imanaka , J. Phys. Chem. 92(1988)7102.
- 22) N. Giordeno, J. C. Bart, A. Vaghi, A. Castellani, G. Mationotti, J. Catal., 36 (1975) 81.
- 23) K. Chen, S. Xie, A. T. Bell, E. Igllesia, J. Catal., 198 (2001) 232.
- 24) H. Hang Chien, I.E.Wachs, J. Phys. Chem., 99 (1995) 10911.
- 25) S.M. Airaksimen, A.O Krause, J. Sainio, J. Lahtinen, M. O. Guerrero-Perez, M.A. Banares, Phys. Chem. Chem. Phys., 5 (2003) 4371.
- 26) B. M. Weckhuysen, I. E. Wachs, R. A. Schoronheydt, Chem. Rev. 96 (1996) 3327.
- 27) M. Benitez, C.A. Quesini, N. S. Figoli, Appl. Catal. A 252 (2003) 427.
- 28) Y.-C. Xie, Y. -Q. Tang, Adv. Catal. 37 I(1990) 1.
- 29) M. C. Abello, M. F. Gomez, L. E. Cadus, Ind. Eng. Chem. Res., 35 (1996) 2137.
- 30) S. Zingg, L.E. Makovsky, R.E. Tisher, F.R. Brown, J. Phys. Chem., 84 (1980) 2998.  
I. E. Wachs, Catal. Today, 45 (1996) 437.
- 31) W.L. Jolly (ed) " Inorganic Synthesis" , XI, MC. Graco, Hill Book Co., New York, 1968, P2.
- 32) S.R. Stampfi, Y. Chen, J. P. Dumesic, C. Niu, C.G. Hill, J. Catal., 105 (1987) 445.
- 33) Cavani, M. Koutyrev, F. Trifiro, A. Bartolini, D. Ghisletti, R. Iezzi, A. Santucci, G. Del Piero, J. Catal.. 158 (1996)236.
- 34) R. L. Puurunen, B. M. Weckhuysen, J. Catal. 210 (2002) 418.
- 35) M.A. Vuurman, I.E. Wachs, D.J. Stufkens, A. Oskam, J. Mol. Catal. A 80 (1993) 209.
- 36) F.D. Hardcastle, I. E. Wachs, J. Mol. Catal. A 46 (1988) 173.
- 37) M.M. Mohamed , S. M. A. Katib, Appl. Catal. A. 287 (2005) 236.
- 38) C.P. Cheng, G. L. Scharader, J. Catal. 60 (1979) 276.
- 39) C. Thomazeau, . Martin, P. Afanasiev, Appl. Catal.,199 (2000) 61.
- 40) J.Leyer, R. Margraf, E. Taglauer, H. Knozing, ur.Sci, 201 (1988) 603.
- 41) N.Radivan, A. Ghozza, G. El-Shobky, Thermochemica Acta, 308 (2003) 211.
- 42) S. Brunauer, L. S. Deming, W. E. Deming, E. E. Teller, J. Am. Chem. Soc. 62 (1940) 1723.
- 43) S. Mathew, C. S. Kumara, N. Nagaraju, J. Mol. Catal. A, 255 (2006) 243.
- 44) R.N. Nickolov, R.M. Edrev-Kardjieva, V.J.Kafedjisky, D.A. Nikolova, N.b. Stankova, D.R. Mehandjiev, Appl. Catal., 190 (2000) 191.
- 45) J.H. De Boer, B.G. Linen, T. J. Osniga, ibid., 4 (1965) 319